

PAPER • OPEN ACCESS

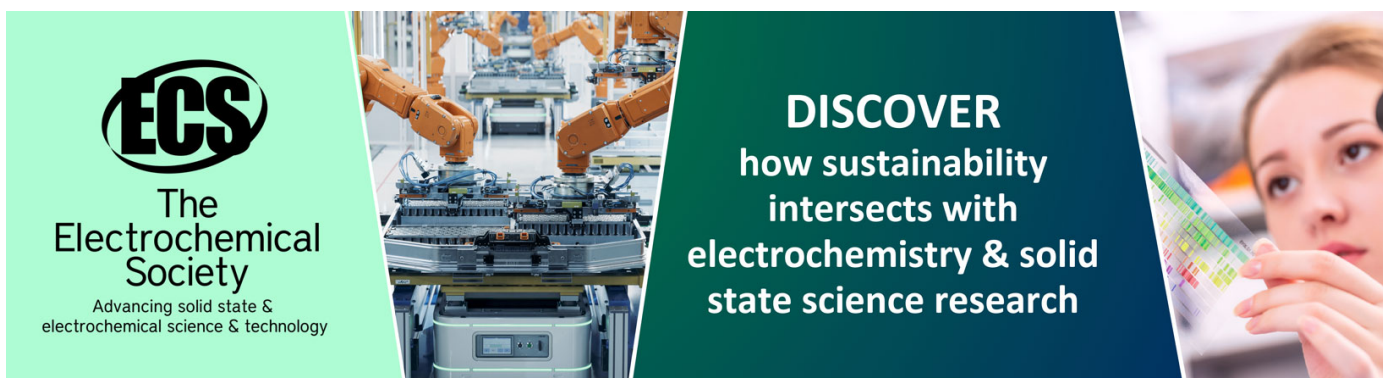
## MEG II physics and detector performance

To cite this article: M. Chiappini on behalf of the MEG II collaboration 2023 *JINST* 18 C10020

View the [article online](#) for updates and enhancements.

You may also like

- [Impact of SQUIDs on functional imaging in neuroscience](#)  
Stefania Della Penna, Vittorio Pizzella and Gian Luca Romani
- [Compliant finger sensor for sensorimotor studies in MEG and MR environment](#)  
Y Li, X Yong, T P L Cheung et al.
- [SQUIDs in biomagnetism: a roadmap towards improved healthcare](#)  
Rainer Körber, Jan-Hendrik Storm, Hugh Seton et al.



**ECS**  
The  
Electrochemical  
Society  
Advancing solid state &  
electrochemical science & technology

**DISCOVER**  
how sustainability  
intersects with  
electrochemistry & solid  
state science research

NEW FRONTIERS IN LEPTON FLAVOR  
PISA, ITALY  
15–17 MAY 2023

## MEG II physics and detector performance

---

### M. Chiappini on behalf of the MEG II collaboration

*INFN Sezione di Pisa,  
Largo B. Pontecorvo 3, 56127 Pisa, Italy*

*E-mail: [marco.chiappini@pi.infn.it](mailto:marco.chiappini@pi.infn.it)*

**ABSTRACT:** In the panorama of the state-of-the-art searches for extremely rare Charged Lepton Flavor Violating (CLFV) processes, the Mu-E-Gamma (MEG) experiment is definitely a reference point in the intensity frontier of modern physics research, setting the best upper limit on the  $\mu^+ \rightarrow e^+\gamma$  decay. The upgrade of MEG, MEG II, wants to give further impetus to the CLFV searches with muons. MEG II relies on a series of upgrades: on the photon side we point up improvements of the  $\gamma$  detector resolutions and acceptance; on the positron side we rely on completely brand new detectors with better acceptance, efficiency and performances; on the Trigger and Data Acquisition (DAQ) side we are able to exploit a higher muon beam intensity despite the increased number of read out channels thanks to a new and optimized electronics. After three years of commissioning, in 2021 the MEG II experiment finally entered the physics data taking phase. An overview of the MEG II physics and experimental contexts is presented, together with the current detector performances based on data. Thanks to the new experimental apparatus the final sensitivity goal is expected to be one order of magnitude better than the first phase of MEG.

**KEYWORDS:** Calorimeters; Particle tracking detectors (Gaseous detectors); Spectrometers; Timing detectors



---

## Contents

<b>1</b>	<b>Introduction</b>	<b>1</b>
<b>2</b>	<b>The MEG II experiment</b>	<b>2</b>
<b>3</b>	<b>Physics data taking and current performances</b>	<b>4</b>

---

## 1 Introduction

**Physics context.** Modern particle physics research can be divided in two main branches: the *energy frontier*, with the search for direct production of new particles at the Large Hadron Collider (LHC at CERN) in the TeV range and the observation of New Physics (NP) interactions Beyond the Standard Model (BSM); the *intensity frontier*, a complementary approach, which exploits precision measurements of extremely rare known processes in order to find deviations from theoretical predictions. Indirect searches allow to probe, constrain or exclude many physics models simultaneously and find new particles as virtual ones in t-channel processes. Ad hoc experiments can indirectly explore highest energy scales, up to  $10^{4-5}$  TeV/c<sup>2</sup>, by exploiting high statistics and well controlled experimental conditions, both unattainable at LHC by general-purpose experiments.

Lepton Flavor Violating (LFV) processes are experimentally observed for neutral leptons in the phenomenon of the neutrino oscillation ( $\nu_l \rightarrow \nu_{l'}$ ). If Lepton Flavor Violation will be observed for charged leptons (Charged Lepton Flavor Violation — CLFV,  $l \rightarrow l'$ ), this will be the definitive evidence of NP BSM. SM extensions including the neutrino oscillations allow CLFV processes, but, due to the very low  $\nu$  mass compared to the  $W$  boson mass, these are not experimentally observable: Branching Ratios  $\text{BR} < 10^{-50}$  [1]. Nevertheless, BSM theories (like Super Symmetry-Grand Unification Theory — SUSY-GUT) predict additional particles and interactions, with LFV-enhancements up to an observable level:  $\text{BR} \sim 10^{-(14-15)}$  [1].

In this context, the MEG experiment represents the state of the art in the search for the CLFV  $\mu^+ \rightarrow e^+\gamma$  decay. The final MEG (phase 1) result, exploiting the full statistics collected during the 2009–2013 data taking period at the Paul Scherrer Institut (PSI, Switzerland), sets the world best upper limit  $\text{BR}(\mu^+ \rightarrow e^+\gamma) < 4.2 \times 10^{-13}$  at 90% Confidence Level [2]. An upgrade of the MEG experiment, MEG II, was designed and it is presently in the physics data taking phase at PSI, aiming at a sensitivity level of  $6 \times 10^{-14}$ . Thus, in terms of NP reach, MEG II is competitive with the new generation of CLFV experiments.

**The  $\mu^+ \rightarrow e^+\gamma$  decay.** In the MEG II experimental apparatus a high intensity continuous  $\mu^+$  beam (rate up to  $R_\mu = 10^8$  Hz) is stopped in a thin target, so the muons decay at rest. The  $\mu^+ \rightarrow e^+\gamma$  process is fully characterized by four kinematic variables: the positron  $E_e$  and photon  $E_\gamma$  energies; the  $e^+ - \gamma$  relative time  $t_{e\gamma}$  and angle  $\theta_{e\gamma}$ . Following the 2-body kinematics and being  $m_\mu$  the muon mass, the signal has  $E_e = E_\gamma = m_\mu/2$ ,  $t_{e\gamma} = 0$  s,  $\theta_{e\gamma} = 180^\circ$ .

Two sources of backgrounds can mimic the signal: the Radiative Muon Decay (RMD)  $\mu^+ \rightarrow e^+ \nu_e \bar{\nu}_\mu \gamma$ , featuring  $E_e < m_\mu/2$ ,  $E_\gamma < m_\mu/2$ ,  $t_{e\gamma} = 0$  s,  $\theta_{e\gamma} < 180^\circ$ ; the accidental coincidence of a positron from the standard muon decay  $\mu^+ \rightarrow e^+ \nu_e \bar{\nu}_\mu$  and a photon from RMD, Annihilation-In-Flight (AIF) and bremsstrahlung processes, featuring  $E_e < m_\mu/2$ ,  $E_\gamma < m_\mu/2$ ,  $t_{e\gamma} = \text{flat}$ ,  $\theta_{e\gamma} < 180^\circ$ . The accidental rate scales with the square of  $R_\mu$  [3]:  $R_{\text{ACC}} = R_\mu \times B_{\text{ACC}} \approx R_\mu^2 \delta E_e \delta t_{e\gamma} (\delta E_\gamma)^2 (\delta \theta_{e\gamma})^2$ , indicating with  $\delta$  the experimental resolutions on the kinematic variables and with  $B_{\text{ACC}}$  the probability that a background event is recognized as signal. The RMD background rate scales only linearly with  $R_\mu$ :  $R_{\text{RMD}} = R_\mu \times \text{BR}_{\text{RMD}}$ . In a high rate environment, like MEG II, the accidental background is dominant by approximately one order of magnitude.

## 2 The MEG II experiment

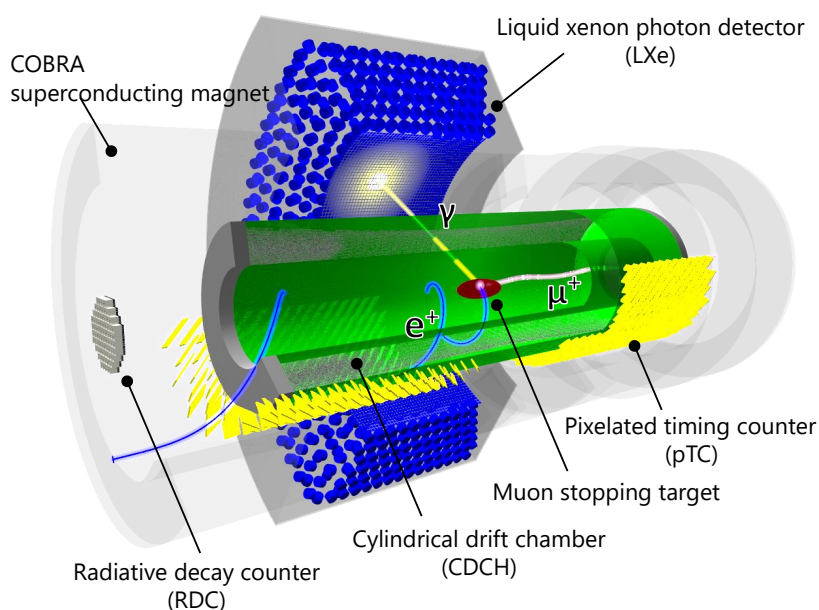


**Figure 1.** Schematic view of the MEG II experimental apparatus with a drawing of a signal  $\mu^+ \rightarrow e^+ \gamma$  event.

**Experimental apparatus.** PSI hosts the world’s most powerful High Intensity Proton Accelerator (HIPA) which drives several user facilities, including the Swiss Muon Source (S $\mu$ S), the world’s most intense continuous muon source. A proton beam (kinetic energy of 590 MeV) impinges on a graphite target and the resulting surface muons (momentum of 28 MeV/c) are collected by the  $\pi$ E5 beam line and driven to the MEG II apparatus [4] (figure 1), surrounding the 174  $\mu\text{m}$ -thick,  $15^\circ$ -slanted  $\mu^+$  stopping target, made of scintillator material (BC-400). Dedicated high-resolution detectors with high rate capability are designed to measure the  $\mu^+ \rightarrow e^+ \gamma$  kinematic variables.

On the positron side, the magnetic spectrometer is placed inside the COBRA (COntant Bending RAdius) superconducting gradient-field (1.27–0.49 Tesla) magnet. It is formed by two completely brand new detectors. A pixelated Timing Counter (pTC) [5], featuring scintillator tiles (BC-422,  $L \times W \times T = 120 \times (40 \text{ or } 50) \times 5 \text{ mm}^3$ , with a  $45^\circ$  tilt angle to be approximately perpendicular to  $e^+$  trajectories) read out by Silicon Photo-Multipliers (6 SiPMs per tile side with

series connection) measures the positron time with a resolution of  $\sim 40$  ps. The pTC is made of 2 semi-cylindrical super-modules mirror symmetric to each other and placed Up-Stream (US) and Down-Stream (DS) of the stopping target. Each super-module hosts 256 counters (16 counters @5.5 cm interval in  $z$  and 16 counters @ $10.3^\circ$  interval in  $\phi$ ), ensuring the full  $e^+$  angular acceptance coverage ( $23 \text{ cm} < |z| < 116.7 \text{ cm}$ ,  $-165.8^\circ < \phi < +5.2^\circ$ ) with the  $\gamma$  pointing to the C-shape photon detector (see below).

A low-mass ( $1.6 \times 10^{-3} X_0$ ), single volume (length and diameter of 2 m and 60 cm respectively) Cylindrical Drift Chamber (CDCH) [6] with high granularity (9 layers of 192 drift cells, few mm wide, defined by 11904 wires) measures the positron momentum vector, with position, angular and momentum resolutions at 1 mm, 6.5 mrad and 100 keV/c level respectively. The CDCH ensures the full azimuthal coverage around the target with an active region which starts and extends radially at  $R \sim 20$  cm and for  $\Delta R \sim 8$  cm respectively ( $\sim 14$  cm bending radius of signal  $e^+$ ). The drift cells are quasi-square with a  $20 \mu\text{m}$  gold-plated tungsten sense wire surrounded by  $40/50 \mu\text{m}$  silver-plated aluminum field wires (5:1 field-to-sense wires ratio). The wires are not parallel to the axis, but form an angle varying from  $6^\circ$  in the innermost layer (L9) to  $8.5^\circ$  in the outermost layer (L1). This stereo angle has an alternating sign, depending on the layer, allowing the reconstruction of the longitudinal hit coordinate  $z$ . The gas mixture is He: $i\text{C}_4\text{H}_{10}$  (90:10) + additives to reach the operational stability. The High-Voltage (HV) Working Point (WP) ranges from 1400 V (L9) to 1480 V (L1).

On the photon side, the C-shape cryostat of the biggest Liquid Xenon (LXe) detector in the world (900 liters) [7] is placed outside COBRA. It measures the photon energy, time and interaction point, featuring a new improved double readout: 4096 SiPMs on the entrance face + 846 PMTs on the other faces. Thanks to the lower material budget and increased light collection uniformity and acceptance with respect to the MEG layout, the energy and position resolutions are expected to be at 1% and a few mm level respectively. A new additional detector, the Radiative Decay Counter (RDC), is placed DS of the target along the beam axis to tag low-energy  $e^+$  (1–5 MeV) from AIF/RMD in time coincidence with high-energy  $\gamma$  ( $> 48$  MeV) to reduce the background. An impact in the MEG II sensitivity up to 15% is expected. It is made of 12 BC-418 plastic scintillators + 76 LYSO crystals for time and energy measurements at 100 ps and 8% level respectively.

The re-design of the MEG II detector led to an increase of a factor 3 in the number of readout channels ( $\sim 9000$ ). The Trigger and DAQ operations were then integrated in a new and optimized single system, the WaveDAQ [8]. It is formed by 37 custom crates each housing: 16 WaveDREAM (WD) DAQ Boards (16 channels each) + 1 Trigger Concentrator Board (TCB) for online data processing and clock and trigger signals distribution + 1 Data Concentrator Board (DCB) for data handling/formatting. In order to suppress the background offline, the whole waveform is acquired at 1.4 GSPS. A digitization with 80 MHz ADCs is used to execute complex trigger algorithms with the integrated FPGA. The online resolutions on  $E_\gamma$  and  $t_{e\gamma}$  are expected to be at 2.5% and 2 ns level respectively with the final trigger rate in the 10–30 Hz range.

**Main problems and solutions.** Two main problems occurred during the construction and commissioning of the CDCH. The first one is the breaking of 107 Al(Ag) cathode wires. After deep investigations [9], the origin of the breaking was found to be the galvanic corrosion of the Al core caused by the air moisture condensation inside cracks in the Ag coating. A good linear correlation between the number of broken wires and exposure time to humidity was found. The problem was

then fully cured by keeping the CDCH volume in an inert atmosphere. In order to avoid random shorts leading to not operational sectors of the detector, a dedicated high-precision tool was built and all the broken wire pieces were extracted from the chamber.

The second problem occurred during the detector operation in 2019, after an accidental anode-cathode short circuit. An anomalous increase in current, up to  $I \sim 400 \mu\text{A}$ , during nominal operations was observed. In order to understand the problem, the external carbon fiber support structure was replaced by a transparent Plexiglas shell and dedicated HV tests with the standard gas mixture were performed. Corona-like discharges were directly spotted in correspondence of six whitish regions on the wires.<sup>1</sup> Accelerated ageing tests on prototypes returned no design issues or discharges. A dedicated optimization of the gas mixture was then started in 2020, trying several additives to recover the normal detector operation. During a conditioning period, the initially high currents, resulting from the  $e^+$  ionization at increasing  $\mu^+$  beam intensity ( $R_\mu$ ), were lowered by adding Oxygen to the gas mixture, up to 2%. Once recovered the  $I$  vs.  $R_\mu$  proportionality, the  $\text{O}_2$  content was gradually reduced to 0.5% to avoid attachment effects. In addition, isopropyl alcohol proved to be crucial to keep the stability in the current level. The CDCH is now operated at the HV WP in stable conditions at full MEG II beam intensity with the standard gas mixture + isopropyl alcohol (1.5%) +  $\text{O}_2$  (0.5%). The measured stable current (10–20  $\mu\text{A}$  range) translated in accumulated charge/cm is in agreement with the design value:  $\sim 0.1 \text{ C/year/cm}$ . The measured gas gain  $G = (2-4) \times 10^5$  is in agreement with the expectation.

The LXe detector was operated since 2017. A continuous decrease of the SiPM Photon Detection Efficiency/Quantum Efficiency (PDE/QE) was experienced. After several investigations [10], the cause was found is the SiPM surface damage by radiation. The PDE recovery was successfully achieved by performing an annealing procedure, consisting in heating the SiPMs by applying a reverse bias with a dedicated power supply (Joule heat method). About two months are needed to complete the annealing of all the sensors, reaching at least  $\sim 15\%$  PDE, a factor of three recovery. This value allows to operate the LXe at full MEG II beam intensity for a full DAQ year (about 120 days). Then, this procedure is repeated every year during the accelerator shutdown period.

### 3 Physics data taking and current performances

After three intense years of commissioning [11], with all the sub-detectors installed and the full DAQ electronics available for the first time in 2021, the MEG II physics data taking period officially started in 2021 and it is currently ongoing. The sensitivity goal  $\text{BR}(\mu^+ \rightarrow e^+\gamma) \sim 6 \times 10^{-14}$  is expected to be reached in five years (2026). The current detector performances [12], compared to the expected ones [13], are summarized in table 1. On the left the Gaussian  $\sigma$  resolutions are displayed: positron energy, angle and position (at the target); photon energy (for shallow/deep  $\gamma$  interaction points inside the LXe) and interaction point inside the LXe (transverse  $(u, v)$  and depth  $w$  coordinates); combined  $e^+ - \gamma$  relative time. On the right the positron, photon and trigger reconstruction efficiencies are summarized. In 2023 the first result based on the unblinding of the 2021 data set is planned. The combined 2021+2022 data analysis will follow, allowing to reach a result already better than the final MEG result. The following years are expected to be very exciting on the CLFV side.

<sup>1</sup>SEM/EDX analyses highlighted the presence of sulfur traces.



**Table 1.** Current performances of the MEG II experiment.

Resolutions			Efficiency (%)		
	Foreseen	Achieved		Foreseen	Achieved
$E_e$ (keV)	100	89	$\epsilon_e$	65	67
$\phi_e, \theta_e$ (mrad)	3.7/6.7	4.1/7.4	$\epsilon_\gamma$	69	62
$y_e, z_e$ (mm)	0.7/1.6	0.7/2.0	$\epsilon_{\text{TRG}}$	$\approx 99$	80
$E_\gamma$ (%) ( $w \neq 2$ cm)	1.7/1.7	2.0/1.8			
$u_\gamma, v_\gamma, w_\gamma$ (mm)	2.4/2.4/5.0	2.5/2.5/5.0			
$t_{e\gamma}$ (ps)	70	78			

## References

- [1] L. Calibbi and G. Signorelli, *Charged Lepton Flavour Violation: An Experimental and Theoretical Introduction*, *Riv. Nuovo Cim.* **41** (2018) 71 [[arXiv:1709.00294](#)].
- [2] MEG collaboration, *Search for the lepton flavour violating decay  $\mu^+ \rightarrow e^+\gamma$  with the full dataset of the MEG experiment*, *Eur. Phys. J. C* **76** (2016) 434 [[arXiv:1605.05081](#)].
- [3] Y. Kuno and Y. Okada, *Muon decay and physics beyond the standard model*, *Rev. Mod. Phys.* **73** (2001) 151 [[hep-ph/9909265](#)].
- [4] MEG II collaboration, *The design of the MEG II experiment*, *Eur. Phys. J. C* **78** (2018) 380 [[arXiv:1801.04688](#)].
- [5] M. Nishimura et al., *Full system of positron timing counter in MEG II having time resolution below 40 ps with fast plastic scintillator readout by SiPMs*, *Nucl. Instrum. Meth. A* **958** (2020) 162785.
- [6] M. Chiappini et al., *The Cylindrical Drift Chamber of the MEG II experiment*, *Nucl. Instrum. Meth. A* **1047** (2023) 167740.
- [7] S. Kobayashi, *Full Commissioning of Liquid Xenon Scintillation Detector to Search for  $\mu^+ \rightarrow e^+\gamma$  with the Highest Sensitivity in MEG II Experiment*, Ph.D. Thesis, University of Tokyo (2022).
- [8] M. Francesconi et al., *The WaveDAQ integrated Trigger and Data Acquisition System for the MEG II experiment*, *Nucl. Instrum. Meth. A* **1045** (2023) 167542.
- [9] A.M. Baldini et al., *Detailed analysis of chemical corrosion of ultra-thin wires used in drift chamber detectors*, *2021 JINST* **16** T12003 [[arXiv:2108.13948](#)].
- [10] K. Ieki et al., *Study on degradation of VUV-sensitivity of MPPC for liquid xenon scintillation detector by radiation damage in MEG II experiment*, *Nucl. Instrum. Meth. A* **1053** (2023) 168365 [[arXiv:2211.09882](#)].
- [11] MEG II collaboration, *Towards a New  $\mu^+ \rightarrow e^+\gamma$  Search with the MEG II Experiment: From Design to Commissioning*, *Universe* **7** (2021) 466.
- [12] A.M. Baldini et al., *Operation and performance of MEG II detector*, to be submitted *Eur. Phys. J. C* (2023).
- [13] MEG II collaboration, *The Search for  $\mu^+ \rightarrow e^+\gamma$  with 10–14 Sensitivity: The Upgrade of the MEG Experiment*, *Symmetry* **13** (2021) 1591 [[arXiv:2107.10767](#)].